Photodissociation dynamics of formyl fluoride (HFCO) at 193 nm: Branching ratios and distributions of kinetic energy

Shih-Huang Lee, Chia-Yan Wu, Sheng-Kai Yang, and Yuan-Pern Lee

Citation: The Journal of Chemical Physics **123**, 074326 (2005); doi: 10.1063/1.2006093
View online: http://dx.doi.org/10.1063/1.2006093
View Table of Contents: http://scitation.aip.org/content/aip/journal/jcp/123/7?ver=pdfcov
Published by the AIP Publishing

Photodissociation dynamics of formyl fluoride (HFCO) at 193 nm: Branching ratios and distributions of kinetic energy

Shih-Huang Lee[a),b)]
National Synchrotron Radiation Research Center (NSRRC), 101 Hsin-Ann Road, Hsinchu Science Park, Hsinchu 30076, Taiwan

Chia-Yan Wu and Sheng-Kai Yang
Department of Chemistry, National Tsing Hua University, Hsinchu 30013, Taiwan

Yuan-Pern Lee[a),c)]
Department of Applied Chemistry and Institute of Molecular Science, National Chiao Tung University, Hsinchu 30010, Taiwan and Institute of Atomic and Molecular Sciences, Academia Sinica, Taipei 106, Taiwan

(Received 9 June 2005; accepted 29 June 2005; published online 25 August 2005)

Following photodissociation of formyl fluoride (HFCO) at 193 nm, we detected products with fragmentation translational spectroscopy utilizing a tunable vacuum ultraviolet beam from a synchrotron for ionization. Among three primary dissociation channels observed in this work, the F-elimination channel HFCO→HCO+F dominates, with a branching ratio ~0.66 and an average release of kinetic energy ~55 kJ mol^{-1}; about 17% of HCO further decomposes to H+CO. The H-elimination channel HFCO→FCO+H has a branching ratio ~0.28 and an average release of kinetic energy ~99 kJ mol^{-1}; about 21% of FCO further decomposes to F+CO. The F-elimination channel likely proceeds via the S_1 surface whereas the H-elimination channel proceeds via the T_1 surface; both channels exhibit moderate barriers for dissociation. The molecular HF-elimination channel HFCO→HF+CO, correlating with the ground electronic surface, has a branching ratio of only ~0.06; the average translational release of 93 kJ mol^{-1}, ~15% of available energy, implies that the fragments are highly internally excited. Detailed mechanisms of photodissociation are discussed. © *2005 American Institute of Physics*. [DOI: 10.1063/1.2006093]

I. INTRODUCTION

The dissociation dynamics of formyl fluoride (HFCO) is important, partly because HFCO, a major degradation product of hydrofluorocarbon refrigerant HFC-134a (CF_3CFH_2), plays an important role in the destruction of ozone in the atmosphere,[1–3] and partly because it presents a prototype for studying multichannel unimolecular dissociation and can be compared with the well-investigated system of formaldehyde (H_2CO).[4]

Although there have been extensive experimental and theoretical investigations on photodissociation of HFCO, a complete understanding of its photodissociation dynamics is still lacking. Several decomposition channels are energetically accessible upon excitation of HFCO with ultraviolet (UV) light,

$$\mathrm{HFCO} \rightarrow \mathrm{HF}(X\,^1\Sigma^+) + \mathrm{CO}(X\,^1\Sigma^+) \quad \Delta H_0 = -7.3\ \mathrm{kJ\ mol^{-1}}, \tag{1}$$

$$\rightarrow \mathrm{H}(^2S) + \mathrm{FCO}(X\,^2A') \quad \Delta H_0 = 423.0\ \mathrm{kJ\ mol^{-1}}, \tag{2}$$

$$\rightarrow \mathrm{F}(^2P) + \mathrm{HCO}(X\,^2A') \quad \Delta H_0 = 499.5\ \mathrm{kJ\ mol^{-1}}, \tag{3}$$

$$\rightarrow \mathrm{H}(^2S) + \mathrm{F}(^2P) + \mathrm{CO}(X\,^1\Sigma^+) \quad \Delta H_0 = 563.4\ \mathrm{kJ\ mol^{-1}}, \tag{4}$$

in which enthalpies of reaction at 0 K, ΔH_0, were derived from enthalpies of formation $\Delta H_{0,f}$ in the literature, as listed in parentheses with units kJ mol^{-1} following each species: HFCO(−376.56), HF(−273.3), CO(−110.53), H(217.998), FCO(−171.5), F(79.39), and HCO(43.5).[5] Uncertainties in $\Delta H_{0,f}$ of FCO might be as large as ±18 kJ mol^{-1} because reported values range from −(153±12) to −(184.5±2) kJ mol^{-1}.[6–9]

Channel (1) is expected to proceed on the ground electronic surface. Klimek and Berry observed laser emission of HF upon photolysis of HFCO with UV light of wavelength greater than 165 nm; an average vibrational energy of 42±13 kJ mol^{-1} for HF was estimated.[10] Ishikawa *et al.* detected unresolved infrared emission of HF, but not of CO, when they performed infrared multiphoton decomposition (IRMPD) of HFCO.[11] Choi and co-workers employed stimulated emission pumping (SEP) to prepare highly internally excited HFCO in its ground electronic state and investigated its state-selective dissociation dynamics.[12–16] By comparison of unimolecular rates of dissociation predicted with Rice-Ramsperger-Kassel-Marcus (RRKM) calculations with those determined experimentally as a function of vibrational energy, they estimated a barrier height for the molecular dissociation channel of HFCO to be 205±17 kJ mol^{-1},[15] similar to a barrier height of 180 kJ mol^{-1} estimated from measurements of thermal decomposition rates of HFCO in the tem-

a)Authors to whom correspondence should be addressed.
b)Electronic mail: shlee@nsrrc.org.tw
c)Electronic mail: yplee@mail.nctu.edu.tw

perature range of 1160-1480 K.[17] Choi and co-workers reported that, following state-selective preparation of HFCO in the energy region of 2000–3000 cm^{-1} above the dissociation threshold with SEP, about 20% of available energy was released as rotational energy of CO; product CO observed with laser-induced fluorescence (LIF) showed that $15 \leqslant J \leqslant 63$; depending on the initial dissociative state, $J=45-50$ has the greatest population. They estimated that ~50% of available energy was released as translational energy, based on observed average Doppler widths of LIF lines of CO.[16]

The existence of atomic elimination channels was proposed by Weiner and Rosenfeld,[18] who photolyzed HFCO at 248 and 193 nm and probed CO with time-resolved laser absorption. Following excitation of HFCO at 248 nm, "late" CO ($v=0-2$) was formed with a rate $\sim 10^4\ s^{-1}$; they ascribed it to a mechanism of formation via decomposition of a partially vibrationally relaxed primary product, either FCO or HCO. In contrast, excitation of HFCO at 193 nm results in the formation of prompt CO ($v=0-2$) and late CO ($v=0-4$); formation of the former might indicate the existence of channel (4).

Detailed investigations on radical channels (2) and (3) were performed by the Bristol group.[19–23] They employed H (Rydberg)-atom photofragment translational spectroscopy to investigate photodissociation dynamics of HFCO in the wavelength region of 218.4-248.2 nm and determined a precise dissociation energy of $418.04 \pm 0.24\ kJ\ mol^{-1}$ for the C-H bond; this channel [reaction (2)] has an estimated appearance threshold ~56.7 $kJ\ mol^{-1}$ above the energy of H+FCO and is correlated with the triplet surface.[22] An additional feature due to H atoms with greater kinetic energy, observed for $\lambda < 233$ nm, was attributed to secondary photolysis of HCO fragment formed via channel (3); the energy of the C-F bond was erroneously estimated as ~377 $kJ\ mol^{-1}$.[22] Further experiments and a reanalysis yielded a revised estimate of an upper limit of 482 $kJ\ mol^{-1}$ for the dissociation energy of the C-F bond; this channel was proposed to proceed also via the triplet surface of HFCO with a small barrier.[23]

Most theoretical workers concentrated on the ground electronic state of HFCO.[24–34] The barrier of channel (1) was calculated to be in the range of $180-197\ kJ\ mol^{-1}$,[27–30] consistent with experiments.[15,17] Yamamoto and Kato employed classical trajectory calculations to predict internal-state distribution of products HF and CO in channel (1); HF is significantly vibrationally excited, whereas CO is rotationally excited.[29] Anand and Schlegel performed similar calculations on photolysis of HFCO and HClCO and reached similar conclusions on the internal distribution of fragments CO and HF; the translational release was predicted to be about 42% of the available energy.[33] Sumathi and Chandra investigated decomposition of HFCO in its lowest triplet (T_1) state $a\ ^3A''$ with an unrestricted Hartree-Fock method, UHF/6-31G*/UMP2, and predicted that triplet HFCO might decompose to H+FCO, but not F+HCO, because the barrier for the latter channel is high.[35] Tachikawa performed direct *ab initio* calculations on the dissociation dynamics of triplet HFCO and predicted energy partitioning of channels (2) and (3); he also predicted that the barrier of channel (2) is significantly smaller than that of channel (3).[36] Fang and Liu employed a complete-active-space self-consistent-field (CASSCF) method to investigate the dissociation dynamics on the three lowest electronic states ($X\ ^1A'$, $a\ ^3A''$, and $A\ ^1A''$) of HFCO and predicted that the mechanism for C-H bond cleavage [channel (2)] is via intersystem crossing from the $A\ ^1A''$ state to the $a\ ^3A''$ state, followed by decomposition on the $a\ ^3A''$ surface, consistent with experimental results.[37] In contrast, they found that the cleavage of the C-F bond might proceed via the T_1 surface, as proposed in previous experimental work,[23] and directly via the $A\ ^1A''(S_1)$ surface.[23]

We report here investigation of photodissociation dynamics of HFCO at 193 nm with photofragment translational spectroscopy using tunable vacuum ultraviolet photoionization for product detection. Both H- and F-elimination channels followed by secondary decomposition and the HF-molecular elimination channel were observed; their branching ratios and kinetic-energy release were determined.

II. EXPERIMENTS

The experimental apparatus is described in detail elsewhere;[38–40] only a brief description is given here. Photofragment time-of-flight (TOF) spectra were measured in a molecular-beam apparatus coupled with radiation from a synchrotron as a source for VUV ionization. The molecular-beam machine comprises two rotatable source chambers, a reaction chamber, a quadrupole mass filter, and a Daly-type ion counter. A sample cell containing HFCO was kept in a slush (211 K) of dry ice mixed with acetone to yield vapor at a pressure of ~68 Torr. We used argon to carry the vapor of HFCO; a stagnation pressure of ~250 Torr for expansion was employed and no clustering was observed under such conditions. An ArF excimer laser beam at 193 nm was directed into the reaction chamber and crossed the molecular-beam perpendicularly. To avoid multiphoton absorption, we decreased the photon intensity to 2-4 mJ/pulse and focused it into a size of $2 \times 8\ mm^2$ at the reaction region. The pressure of the reaction chamber was maintained below 2×10^{-8} Torr so that a collision-free condition was achieved. After a free flight along a path of length 100 mm, photofragments were ionized with synchrotron radiation emitted from an undulator; the fundamental photon energy is readily tunable on adjusting the gap of the undulator. The energy resolution ($\Delta E/E$) of the resultant VUV beam is ~3%. To gain photon flux ($\sim 1 \times 10^{16}$ photons s^{-1}) sufficient to ionize reaction products, we employed a windowless gas filter in the beam line in place of a monochromator to suppress the harmonic photons from the undulator; depending on the desired photon energy, we flowed Ne, Ar, or Kr through the filter. The VUV beam was reflected into the ionization region of the molecular-beam machine with a focusing mirror. The ionization region was evacuated to 5×10^{-12} Torr. The ion signal due to synchrotron radiation alone, i.e., without the photolysis light, was subtracted from the raw TOF spectra. TOF spectra were accumulated over $(2\text{-}14) \times 10^5$ laser shots to achieve sufficient ratio of signal to noise.

HFCO was synthesized by reacting anhydrous formic acid with KHF_2 and benzoyl chloride[41] and purified with

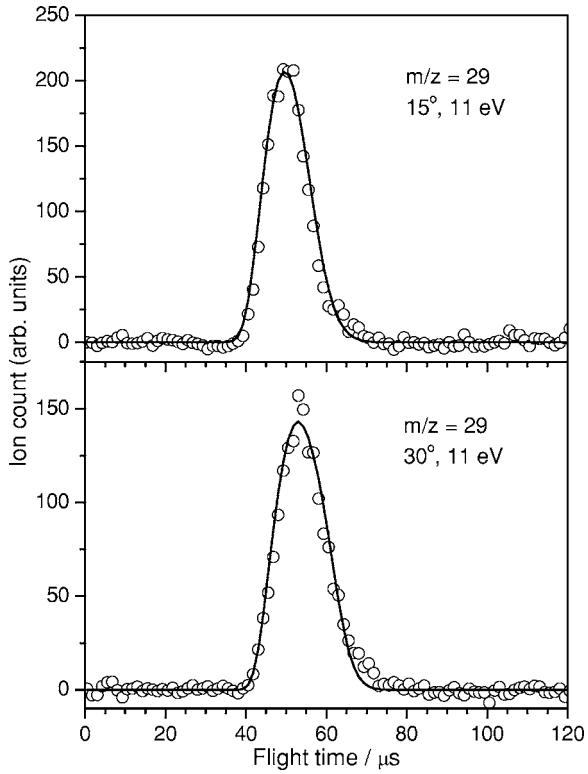

FIG. 1. Time-of-flight spectra for m/z 29 (HCO) detected at laboratory angles 15° and 30° using ionizing photons at 11 eV. The simulated curves are shown as solid lines.

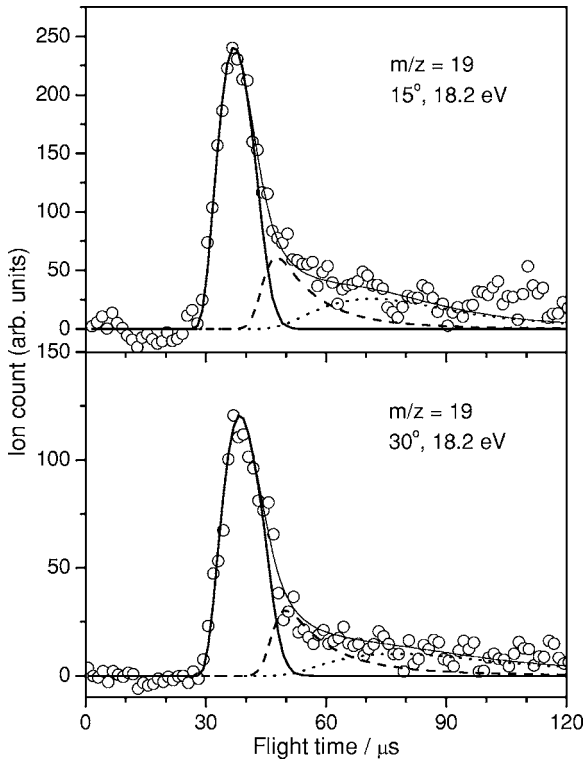

FIG. 2. Time-of-flight spectra for m/z 19 (F) detected at laboratory angles 15° and 30° using ionizing photons at 18.2 eV. Experimental data are deconvoluted into three components corresponding to channels (3′) (F+HCO, solid line), (3″) (F+HCO with secondary dissociation of HCO, dashed line), and (2″) (H+FCO with secondary dissociation of the FCO, dotted line), respectively.

several trap-to-trap distillations before being stored at 77 K before use. The purity of HFCO, tested with infrared-absorption spectroscopy, exceeded 99%.

III. RESULTS AND ANALYSIS

The photodissociation laser was unpolarized, hence producing an isotropic angular distribution of photofragments around the laser beam. The center-of-mass translational energy distribution $P(E_t)$ was obtained from the TOF spectra using a forward convolution technique that involves iterative convolution of a trial $P(E_t)$ to generate a simulated TOF spectrum. A computer program (PHOTRAN) served to fit product TOF spectra for binary decomposition, whereas a simulation program (CMLAB3) served to treat the complicated three-body dissociation as a sequential process. All three primary channels were observed upon photolysis of HFCO at 193 nm, as discussed below.

A. Elimination of atomic fluorine

TOF spectra of m/z 29 (HCO) recorded at photoionization energy of 11.0 eV and at scattering angles 15° and 30° are shown in Fig. 1; they are fitted satisfactorily with a single component, and are readily associated with reaction (3), the F-elimination channel. TOF spectra of m/z 19 (F) recorded at photoionization energy of 18.2 eV and at scattering angles 15° and 30° are shown in Fig. 2; they are partitioned into three components—a major sharp feature with large kinetic energy (solid line), a medium feature with less kinetic energy (dashed line), and a weak feature with the least kinetic energy (dotted line). The former two components (solid and dashed lines) comprise the primary dissociation channel HFCO→HCO+F, with the first correlating with HCO that survives [reaction (3′)] and the second with secondary dissociation of HCO due to internal excitation [reaction (3″)],

$$\mathrm{HFCO} \rightarrow \mathrm{F}(^2P) + \mathrm{HCO}(X\,^2A', \text{no further decomposition}), \tag{3'}$$

$$\mathrm{HFCO} \rightarrow \mathrm{F}(^2P) + \mathrm{HCO}^*(X\,^2A') \rightarrow \mathrm{F}(^2P) + \mathrm{H}(^2S) + \mathrm{CO}(X\,^1\Sigma^+), \tag{3''}$$

in which HCO^* denotes internally excited HCO that is produced from reaction (3) and subsequently dissociates. The third, weak component (dotted line) corresponds to secondary dissociation of internally excited FCO, to be discussed in Sec. III D.

Figure 3 shows the $P(E_t)$ derived from the two faster components in TOF spectra of atomic F; the solid-line component of $P(E_t)$ predicts a TOF spectrum of HCO satisfactorily, indicating that this feature is associated with channel (3′). The dashed-line portion with small kinetic energy, hence large internal energy for HCO, corresponds to channel (3″).

B. Elimination of atomic hydrogen

TOF spectra of m/z 47 (FCO) recorded at photoionization energy of 11.8 eV and at scattering angles 15° and 30° are shown in Fig. 4; they are fitted satisfactorily with a single

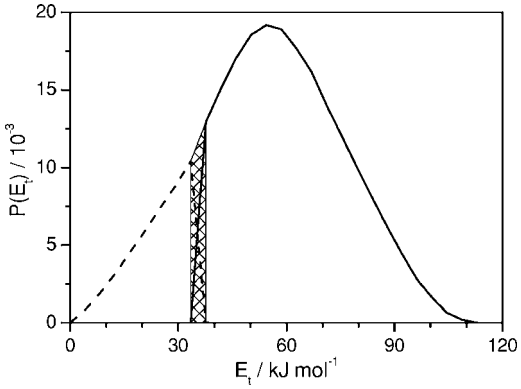

FIG. 3. Kinetic-energy distributions $P(E_t)$ of the F-elimination channel. The hatched area indicates the uncertainty in determining the threshold of secondary dissociation of HCO to produce H+CO.

component, and are readily associated with reaction (2), the H-elimination channel. Because the velocity of FCO is small in the center-of-mass frame after coupling with the velocity of the molecular beam, the backward part of FCO is observable at small laboratory angles. The TOF spectrum of m/z 1 (H) recorded at photoionization energy of 14.8 eV and at a scattering angle 45° is shown in Fig. 5; it is partitioned into three components—two complementary features (solid and dashed lines) with large kinetic energies and a broad feature (dotted line) with less kinetic energy.

The $P(E_t)$ derived from TOF spectra of FCO predicts a TOF spectrum of H atoms matching the observed sharp feature (solid line), indicating that this feature is associated with reaction (2′),

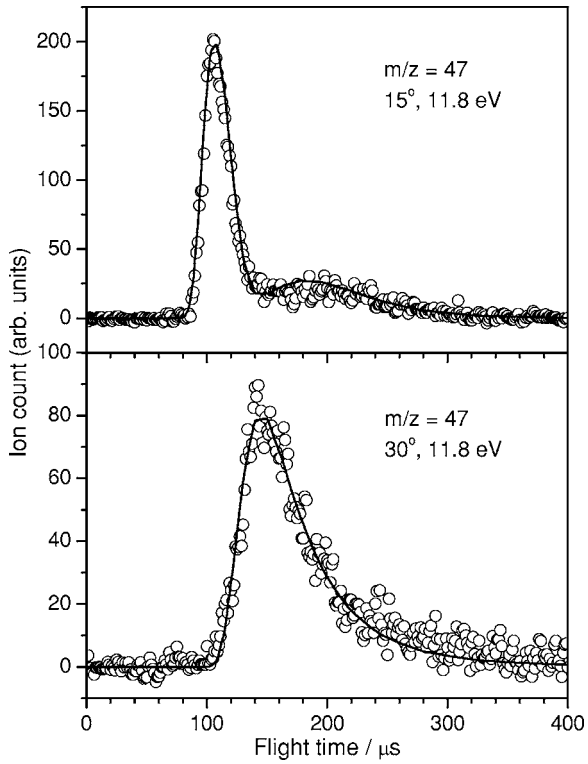

FIG. 4. Time-of-flight spectra for m/z 47 (FCO) detected at laboratory angles 15° and 30° using ionizing photons at 11.8 eV. The simulated curves are shown as solid lines.

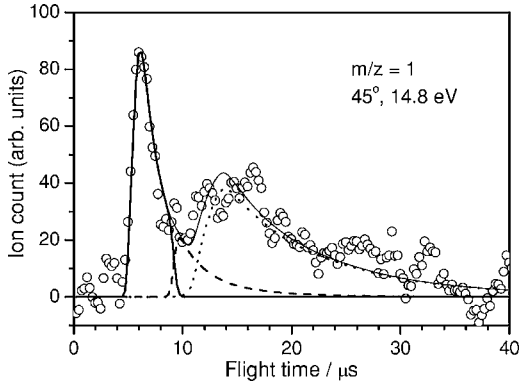

FIG. 5. Time-of-flight spectrum for m/z 1 (H) detected at a laboratory angle 45° using ionizing photons at 14.8 eV. Experimental data are deconvoluted into three components corresponding to channels (2′) (H+FCO, solid line), (2″) (H+FCO with secondary dissociation of FCO, dashed line), and (3″) (F+HCO, with secondary dissociation of HCO, dotted line), respectively.

$$\mathrm{HFCO} \rightarrow \mathrm{H}(^2S) + \mathrm{FCO}(X\,^2A', \text{no further decomposition}). \quad (2')$$

Figure 6 shows the $P(E_t)$ derived from the two faster components in TOF spectra of atomic H; the solid component corresponds to channel (2′). The dashed-line portion with small kinetic energy, hence large internal energy for FCO, corresponds to channel (2″),

$$\begin{aligned}\mathrm{HFCO} &\rightarrow H(^2S) + \mathrm{FCO}^*(X\,^2A') \\ &\rightarrow \mathrm{H}(^2S) + \mathrm{F}(^2P) + \mathrm{CO}(X\,^1\Sigma^+), \end{aligned} \quad (2'')$$

in which FCO^* denotes internally excited FCO that is produced from reaction (2) and subsequently dissociates. The broad feature of H atoms with less kinetic energy is associated with secondary decomposition of HCO fragment produced via F elimination, reaction (3″), to be discussed below. Another broad feature of H atoms with even smaller kinetic energy (not shown in Fig. 5) is ascribed to cracking of HCO^+ because its TOF spectrum may be predicted from the $P(E_t)$ of HCO in Fig. 3.

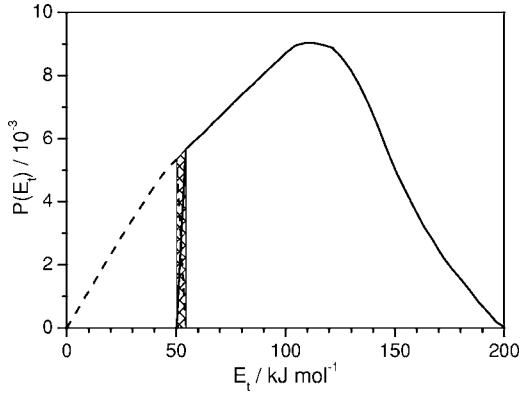

FIG. 6. Kinetic-energy distributions $P(E_t)$ of the H-elimination channel. The hatched area indicates the uncertainty in determining the threshold of secondary dissociation of FCO to produce F+CO.

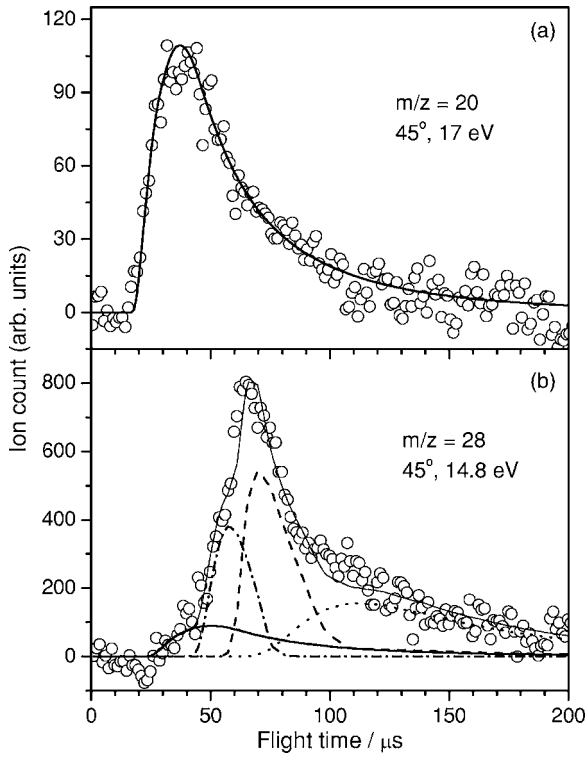

FIG. 7. Time-of-flight spectra for m/z 20 (HF) and 28 (CO) detected at a laboratory angle 45° using ionizing photons at 17 and 14.8 eV, respectively. The TOF spectrum of CO is partitioned into four components corresponding to channel (1) (HF+CO, solid line), cracking of HCO^+ (dot-dashed line), channel (3″) (F+HCO with secondary dissociation of HCO, dashed line) and (2″) (H+FCO with secondary dissociation of FCO, dotted line), respectively.

C. Molecular HF-elimination channel

TOF spectra of m/z 20 (HF) and m/z 28 (CO) at photoionization energies of 17.0 and 14.8 eV, respectively, and at a scattering angle 45° are shown in Fig. 7. The TOF spectrum of HF in Fig. 7(a) is fitted satisfactorily with a single $P(E_t)$, shown in Fig. 8. The TOF spectrum of CO in Fig. 7(b) is partitioned into four components: a rapid, broad feature (solid line), two intense sharp features with slightly less kinetic energy (dpt-dashed and dashed lines), and a broad feature with the least kinetic energy (dotted line). The $P(E_t)$ derived from TOF spectra of HF predicts a TOF spectrum of CO matching the observed rapid, broad feature (solid line in Fig. 7), indicating that this feature is associated with reaction (1). One sharp feature of CO (dot-dashed line) is due to cracking of HCO^+, as its TOF spectrum is predicted from the $P(E_t)$ of HCO in Fig. 3. The other sharp feature of CO (dashed line) is associated with secondary decomposition of internally hot HCO, reaction (3″). The slowest component (dotted line) is associated with secondary decomposition of internally hot FCO, reaction (2″). Both secondary decomposition reactions are discussed in the following Sec. III D.

TOF spectra of CO were recorded at ionization energies ranging from 11.1 to 15.9 eV. The ionization energy of CO is reported to be 14.0142 ± 0.0003 eV,[42] whereas the ionization energy of HCO is 8.14 ± 0.04 eV.[43] At ionization energy of 11.1 eV, CO^+ is produced only from cracking of HCO^+. Using the $P(E_t)$ for the F-elimination channel shown in Fig. 3, we predicted the TOF spectrum of HCO and consequently CO from HCO^+ cracking that fits satisfactorily with experimental observation at ionization energy of 11.1 eV, confirming that the sharp feature of CO (dot-dashed line) in Fig. 7 is due to cracking of HCO^+. At an ionization energy near but smaller than 14 eV, the rapid feature (solid line) in Fig. 7 appears, indicating that some CO fragments produced from channel (1) are also vibrationally excited.

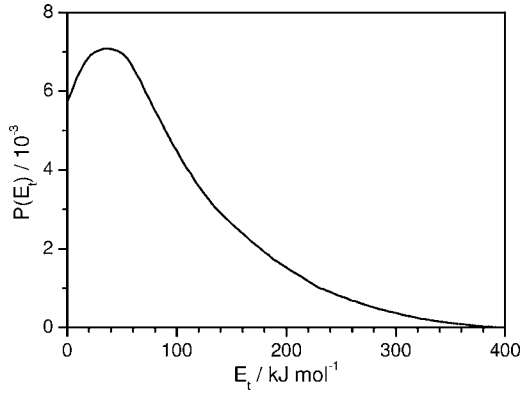

FIG. 8. Kinetic-energy distribution $P(E_t)$ of the HF+CO channel.

Similarly, TOF spectra of HF were recorded at ionization energies ranging from 13.8 to 17.0 eV; the ionization energy of HF is 15.98 ± 0.04 eV.[44] A weak signal of HF^+ was observed at an ionization energy of 13.8 eV, indicating that HF produced from channel (1) might have vibrational energy as much as 2.1 eV (200 kJ mol^{-1}, corresponding to $v=4$ of HF).

D. Secondary decomposition of HCO and FCO

Because some HCO produced upon photodissociation of HFCO has a large internal energy, a fraction of HCO further decomposes into H+CO, resulting in additional features in TOF spectra of CO and H, shown as the dashed line in Fig. 7 and the dotted line in Fig. 5, respectively. An abrupt truncation of a primary $P(E_t)$ indicates that HCO with sufficient internal energy undergoes secondary decomposition before detection. The $P(E_t)$ in Fig. 3 indicates that the threshold for decomposition of HCO is $E_t = 35 \pm 3$ kJ mol^{-1}, corresponding to an exit barrier of 21 ± 3 kJ mol^{-1} and a barrier of $85-102$ kJ mol^{-1} according to literature values of the C-F bond: 499 kJ mol^{-1} from Ref. 5 and 482 kJ mol^{-1} from Ref. 23. The uncertainty of the truncation threshold is represented as hatched area in Fig. 3; the dashed curve represents the original $P(E_t)$ of decomposed HCO.

Similarly, internally excited FCO produced upon photodissociation of HFCO further decomposes into F+CO, resulting in additional features in TOF spectra of CO and F, shown as dotted lines in Figs. 7 and 2, respectively. The $P(E_t)$ in Fig. 6 indicates that the threshold for decomposition is $E_t = 52 \pm 3$ kJ mol^{-1}, corresponding to an exit barrier of 4 ± 3 kJ mol^{-1} and a barrier of $144-149$ kJ mol^{-1} according to literature values of the C-H bond: 423 kJ mol^{-1} from Ref. 5 and 418 kJ mol^{-1} from Ref. 22. The uncertainty of the truncation threshold is represented as hatched area in Fig. 6; the dashed curve represents the original $P(E_t)$ of the decomposed FCO.

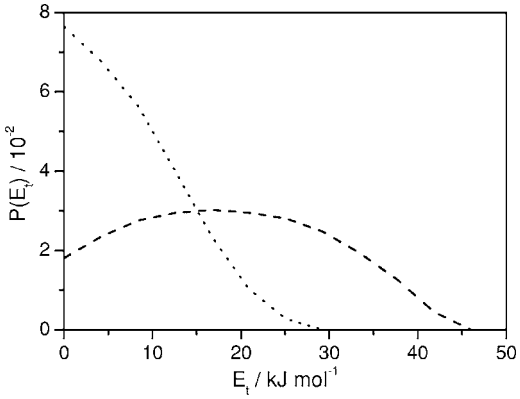

FIG. 9. Kinetic-energy distributions $P(E_t)$ for the secondary dissociation channels HCO→H+CO (dashed line) and FCO→F+CO (dotted line).

Figure 9 shows the kinetic-energy distributions for secondary dissociation processes, HCO→H+CO and FCO →F+CO. The CMLAB3 program serves to simulate TOF spectra of a product after sequential three-body dissociation. The TOF spectra of secondary products atomic H (dotted line in Fig. 5) and CO [dashed line in Fig. 7(b)] can be fitted satisfactorily using the primary $P(E_t)$ (dashed line in Fig. 3), the secondary $P(E_t)$ (dashed line in Fig. 9), and an isotropic angular distribution in the secondary dissociation process. Similarly, the TOF spectra of secondary products atomic F (dotted line in Fig. 2) and CO [dotted line in Fig. 7(b)] can be fitted satisfactorily using the primary $P(E_t)$ (dashed line in Fig. 5), the secondary $P(E_t)$ (dotted line in Fig. 9), and an isotropic angular distribution in the secondary dissociation process.

Available energies, average translational energies of products, and fraction of translational-energy release from various channels are summarized in Table I.

E. Measurements of branching ratios

The branching ratios derived from partitioning of TOF spectra of F, H, and CO are listed in Table II. In Fig. 2, the ratio of rapid F [reaction (3′)], slow F [reaction (3″)], and secondary F [reaction (2″)] is 0.77:0.17:0.06, indicating that direct C-F fission, channel (3), is the major channel relative to other F-producing channels. In Fig. 5, the ratio of the integrated intensity of rapid H [reaction (2′)], slow H [reaction (2″)], and secondary H [reaction (3″)] is 0.57:0.10:0.33. Similarly, partition of the TOF spectrum of CO in Fig. 7 into three features, excluding a fourth one due to cracking of HCO^+, yields a ratio of integrated intensity 0.26:0.37:0.37 for rapid CO [reaction (1)]: medium CO [reaction (2″)]: slow CO [reaction (3″)], indicating that the branching ratio of the molecular elimination of HF is approximately one-third that of CO from secondary decomposition of HCO and FCO. Combining these ratios yields an estimate of the branching ratios 0.06:0.28:0.66 for channels (1)–(3); approximately 21% of FCO and 17% of HCO further decompose to F +CO [reaction (2″)] and H+CO [reaction (3″)], respectively, as listed in the last column of Table II. We have measured the angular anisotropy parameter β of photofragments using linearly polarized laser emission. Two similar TOF spectra of a fragment were observed using polarization parallel and perpendicular to the TOF axis, indicating that photofragments have a nearly isotropic angular distribution with $|\beta|$ smaller than 0.1. As the branching ratios were determined self-consistently without the need of calibration, the uncertainties in determining branching ratios are estimated to be ~10% except for two secondary dissociation channels that might have uncertainties as much as 30%.

IV. DISCUSSION

The first electronically excited singlet (S_1) state $A\ ^1A''$ of HFCO has been characterized experimentally to have a band origin at 37 492 cm^{-1}, corresponding to an energy of 448 kJ mol^{-1}.[45,46] Photoexcitation in the wavelength range of 193–248 nm prepares HFCO in its S_1 state. The only theoretical investigation on dissociation of HFCO in its S_1 state indicates that this state can dissociate to form $F(^2P)$ $+HCO(X\ ^2A')$, channel (3), via a forward potential barrier ~114 kJ mol^{-1}.[37] In contrast, the S_1 state correlates with $H(^2S)+FCO(A\ ^2A'')$ rather than the ground-state products $H(^2S)+FCO(X\ ^2A')$; this dissociation channel is energetically inaccessible for photoexcitation at 193 nm. The first triplet (T_1) state $a\ ^3A''$ of HFCO is predicted to lie ~33 kJ mol^{-1} below the S_1 state[37] and it might dissociate to both $H(^2S)+FCO(X\ ^2A')$ and $F(^2P)+HCO(X\ ^2A')$; predicted barriers for dissociation are ~87 and 119 kJ mol^{-1}, respectively. The ground electronic surface $X\ ^1A'$ of HFCO correlates with both atomic elimination channels (2) and (3) with-

TABLE I. Available energies, averaged kinetic energies, and fractional releases in translational energy for various dissociation channels upon photolysis of HFCO at 193 nm.

Product channel	E_{ava}(kJ mol^{-1})	$\langle E_t \rangle$(kJ mol^{-1})	f_t(%)
(1) HFCO→HF+CO	627	93.3	14.9
(2) HFCO→H+FCO	202[a]	98.7[b]	48.9
(3) HFCO→F+HCO	120–137[c]	54.8[b]	40.0–45.7
(2″) HFCO→H+FCO→H+F+CO	56	[d]34.6+8.1[e]	76.3
(3″) HFCO→F+HCO→F+H+CO	56	[d]24.4+17.5[e]	74.8

[a]Experimental C-H bond energy, 418.0 kJ mol^{-1} (Ref. 22), is used.
[b]Fragments undergoing secondary dissociation are included.
[c]An experimental estimate of an upper limit of the energy of the C-F bond, 482 kJ mol^{-1} (Ref. 23), yields the upper limit of 137 kJ mol^{-1}; see text.
[d]Average kinetic-energy release from primary dissociation.
[e]Average kinetic-energy release from secondary dissociation.

TABLE II. Branching ratios of various product channels upon photolysis of HFCO at 193 nm.

Product channel	From TOF of F (Fig. 2)	From TOF of H (Fig. 5)	From TOF of CO (Fig. 7)	Total branching
(1) HFCO→HF+CO			0.26	0.06±0.01
(2′) HFCO→H+FCO		0.57		0.22±0.02
(2″) FCO→F+CO	0.06	0.10	0.37	0.06±0.02
(3′) HFCO→F+HCO	0.77			0.55±0.05
(3″) HCO→H+CO	0.17	0.33	0.37	0.11±0.02

out a barrier, but the major dissociation channel on this surface has been characterized as HF elimination, channel (1). The barrier of this channel is experimentally estimated to be 180–205 kJ mol^{-1},[15,17] consistent with theoretical calculations.[17,25–27,29] A potential-energy diagram for all dissociation processes based on available information is shown in Fig. 10.

A. The F(^2P)+HCO($X\,^2A'$) channel and secondary decomposition of HCO

Maul *et al.* investigated photodissociation of HFCO at 218.4-248.2 nm by observing TOF spectrum of H atoms using the Rydberg-tagging technique.[23] These authors found signals of H atoms with large kinetic energy and attributed them to secondary photolysis of HCO fragment that were produced from the F+HCO channel; they estimated an upper limit of 482 kJ mol^{-1} for the C-F bond dissociation energy, significantly smaller than the recommended value of 499.5 kJ mol^{-1} based on thermochemical data. Theoretical calculations placed this channel at ~459 kJ mol^{-1} (Ref. 37) and 466 kJ mol^{-1} (Ref. 26) above the energy of HFCO. The available energy for this channel is thus 120–137 kJ mol^{-1}. The exit barrier for this channel on the S_1 surface is predicted to be ~126 kJ mol^{-1}.[37]

The distribution of translational energy for this channel determined in this work (Fig. 3) shows an energy maximum ~112 kJ mol^{-1} and a maximal distribution at energy ~55 kJ mol^{-1}, consistent with available energy and a predicted exit barrier on the S_1 surface. Theoretical calculations predict that this channel can proceed via the S_1 and T_1 surfaces, both with barriers. However, according to RRKM calculations, on the T_1 surface this channel fails to compete with the H+FCO channel that has a smaller barrier. As this is the major channel for dissociation of HFCO at 193 nm, we believe that direct dissociation on the S_1 surface is the most likely mechanism for the production of HCO+F upon photolysis at 193 nm.

The observed secondary dissociation of HCO with a threshold of E_t=35±3 kJ mol^{-1} indicates that the barrier height for this process is 85–102 kJ mol^{-1} with an exit barrier of ~21 kJ mol^{-1}. Observation of a maximum distribution of $P(E_t)$ at ~17 kJ mol^{-1} for this process (Fig. 9, dashed line) is consistent with this potential-energy surface. Kamiya and Morokuma calculated a barrier of 60 kJ mol^{-1} and an exit barrier of 29 kJ mol^{-1} using MP4(SDTQ)/6-311G**//MP2/6-31G*;[26] considering the level of calculations, the agreement between experiments and calculations is satisfactory.

Maul *et al.* observed rapid H atoms due to secondary photolysis of HCO fragments at laser wavelength as large as 248.2 nm and proposed that the C-F dissociation proceeds via the T_1 surface with a dissociation energy less than 482 kJ mol^{-1} and a small barrier. Photolysis of HFCO at 248 nm has energy smaller than the barrier for reaction (3) on the S_1 surface determined in this work. The threshold observed by Maul *et al.* might be associated with the crossing point of the S_1 and T_1 surfaces.

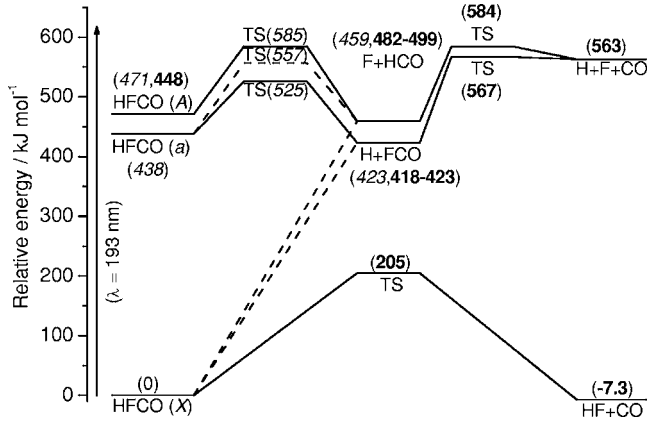

FIG. 10. Schematic of potential-energy surfaces for dissociation of formyl fluoride. Numbers in boldface are experimental results; those from quantum-chemical calculations (Ref. 37) are shown in italic. Energies of transition states (TSS) from F+HCO to F+H+CO and from H+FCO to H+F+CO are determined in this work. The dotted lines indicate three energetically accessible dissociation channels unobserved in this work.

B. The H(^2S)+FCO($X\,^2A'$) channel and secondary decomposition of FCO

The H(^2S)+FCO($X\,^2A'$) channel has been extensively investigated with photofragmentation excitation spectroscopy, Doppler line-shape spectroscopy,[19,21] and Rydberg-tagging spectroscopy.[20,22] The dissociation energy of the C-H bond is determined accurately to be 418.0 kJ mol^{-1}, corresponding to 34 950±20 cm^{-1}; the available energy is thus 201 kJ mol^{-1}.

The distribution of translational energy for this channel that we determined covers the energy range up to ~200 kJ mol^{-1} with a maximal distribution at energy ~113 kJ mol^{-1}, indicating the existence of an exit barrier. Reed *et al.* reported total kinetic-energy release (TKER) spectra of this channel at excitation wavelengths of 246.3, 235.66, 223.34, and 218.4 nm. The TKER spectrum obtained upon photolysis at 218.4 nm covers the range of 24–131 kJ mol^{-1}, with a maximum near 90 kJ mol^{-1}. Our ob-

served distribution of translational energy is consistent with their observation, as the available energy in our experiments is greater by ~72 kJ mol^{-1}. The much improved resolution in Rydberg-tagging spectroscopy enabled observation of structures and a sharp truncation at the high-energy end.[22] We lack the resolution and sensitivity to characterize the structure, and our fitting of the $P(E_t)$ to a smooth curve might result in a fitted upper limit of energy slightly greater than the true value.

Theoretical calculations predict that C-H fission can occur only via the T_1 surface with a barrier, and, according to RRKM theory, this channel is expected to be more important than the C-F fission channel that has a greater barrier. This channel clearly proceeds via intersystem crossing from the S_1 state to the T_1 state before dissociation. The observed most-probable distribution of translational energy at 113 kJ mol^{-1} is consistent with theoretical calculations of an exit barrier of 103 kJ mol^{-1} (Ref. 37). The threshold of 57 kJ mol^{-1}(4740 cm^{-1}) above the energy of H+FCO reported for this channel by Reed *et al.* might be associated with the crossing point of the S_1 and the T_1 surfaces, which was predicted to lie ~51 kJ mol^{-1} above the S_1 state, that is, ~70 kJ mol^{-1} above the energy of H+FCO.

An observed secondary dissociation of FCO with a threshold E_t value of 52±3 kJ mol^{-1} indicates that the barrier height for this process is ~149 kJ mol^{-1} with an exit barrier of ~4 kJ mol^{-1}. Observation of a maximum distribution of $P(E_t)$ near 0 kJ mol^{-1} for this process (Fig. 9, dotted line) is consistent with this potential-energy surface. Kamiya and Morokuma calculated an exit barrier of 13 kJ mol^{-1} using MP4(SDTQ)/6-311G**//MP2/6-31G* for this channel;[26] the agreement between experiment and calculation is satisfactory.

C. The HF+CO channel

The HF+CO channel on the ground electronic surface has been extensively investigated via preparation of a highly internally excited state with SEP.[12–16] They determined a barrier height of 205±17 kJ mol^{-1} for this channel.[15]

Translational-energy distribution for this channel determined in this work covers the energy range of 0–397 kJ mol^{-1} and a maximal distribution at energy ~42 kJ mol^{-1}, indicating the existence of an exit barrier. An observed average kinetic energy of 93 kJ mol^{-1} is slightly smaller than the average energy of 117 kJ mol^{-1} observed by Choi and Moore upon excitation of HFCO to a vibrationally excited state with energy ~234 kJ mol^{-1}.[16] The translational-energy release is dependent mainly on the exit barrier, not the excess energy above the barrier. This channel clearly proceeds via the S_0 state; the S_0 state may be produced via either internal conversion from the S_1 state or intersystem crossing from the T_1 state. According to theoretical calculations, the $S_1 \rightarrow S_0$ crossing point is energetically inaccessible at 193 nm; a plausible mechanism for the direct crossing $S_1 \rightarrow S_0$, if available, would result from vibronic coupling interaction between these two states.

According to the energy balance, upon excitation of HFCO at 193 nm, fragments HF and CO in this channel are expected to be highly internally excited with average internal energy exceeding 500 kJ mol^{-1}. However, Klimek and Berry estimated that only 7% of available energy goes to vibrational energy of HF,[10] and Weiner and Rosenfeld observed CO up to only $v=2$ for prompt CO.[18] Choi and Moore reported that 20% of available energy was released as rotational energy of CO and about 50% to translational energy.[16] Our observation of HF^+ and CO^+ at photon energies smaller than ionization energies of HF and CO indicates that these fragments are vibrationally excited, especially HF. To understand the dynamics on this surface, it is desirable to investigate the internal-energy distribution of both products HF and CO from dissociation of HFCO at 193 nm.

D. Branching ratios

The branching ratios summarized in Table II indicate that the major channel involves C-F fission, with a total branching ratio of 0.66. This value is consistent with our proposal that this channel proceeds via the S_1 surface, thus competing successfully with other channels. The C-H fission channel has a total branching ratio of 0.28, consistent with a mechanism involving intersystem crossing from the S_1 surface to the T_1 surface before dissociation. The HF-elimination channel has a branching ratio of only 0.06, indicating that transformation from the S_1 surface, either directly or indirectly via the T_1 surface, to the S_0 surface is much less facile.

The average internal energies of HCO and FCO are calculated to be about 65-82 and 102 kJ mol^{-1}, respectively, based on observed average kinetic energies of ~55 and 99 kJ mol^{-1} for channels (3) and (2), respectively. The fractions of HCO and FCO that undergo secondary dissociation are 17% and 21%, respectively. Hence the dissociation barrier for FCO is expected to be greater than that of HCO, consistent with our observed energetics and also theoretical predictions.[26] According to our mechanism, the prompt CO observed by Weiner and Rosenfeld[18] might result from secondary dissociation of HCO produced via channel (3″), whereas the slow CO from secondary dissociation of FCO produced via channel (2″) and from HF elimination, channel (1). The branching ratios of CO produced via channels (1), (2″), and (3″)—0.06, 0.06, and 0.11—imply a ratio of ~1:1 for prompt CO to slow CO, consistent with data shown in Fig. 2 of Ref. 18.

V. CONCLUSION

We employed fragmentation translational spectroscopy utilizing a tunable source of vacuum ultraviolet radiation from a synchrotron to investigate the photodissociation dynamics of formyl fluoride (HFCO) at 193 nm. Three primary dissociation channels were observed. The dominant channel, fission of the C-F bond, HFCO→HCO+F, proceeds on the S_1 surface; it has a branching ratio of ~0.66 and an average kinetic-energy release of ~55 kJ mol^{-1}. With excessive internal energy, about 17% of HCO decomposes further to H+CO. The C-H bond fission channel, HFCO→FCO+H, proceeds on the T_1 surface; it has a branching ratio of ~0.28 and an average kinetic-energy release of ~99 kJ mol^{-1}. About

21% of FCO decomposes further to F+CO. Both channels of atomic fission exhibit moderate exit barriers for dissociation. The molecular elimination channel HFCO→HF+CO proceeds via the S_0 surface with a branching ratio of only ~0.06. With an excess energy of 626 kJ mol^{-1}, the average translational-energy release of 93 kJ mol^{-1} indicates that the fragments are highly internally excited. Our work provides a further understanding of the photodissociation dynamics of HFCO at 193 nm and provides a rationale for some previous experimental results.

ACKNOWLEDGMENTS

We thank the National Science Council of Taiwan (Grant No. NSC93-2119-M-009-002 and NSC93-2113-M-213-001) and the National Synchrotron Radiation Research Center for support.

[1] T. J. Wallington, M. D. Hurley, J. C. Ball, and E. W. Kaiser, Environ. Sci. Technol. **26**, 1318 (1992).
[2] A. R. Ravishankara, A. A. Turnipseed, N. R. Jensen, S. Barrone, M. Mills, C. J. Howard, and S. Solomon, Science **263**, 71 (1994).
[3] T. J. Wallington, W. F. Schneider, J. Schested, and O. J. Nelson, Faraday Discuss. **100**, 55 (1995).
[4] X. Li, J. M. Millam, and H. B. Schlegel, J. Chem. Phys. **113**, 218 (2000), and references therein.
[5] M. W. Chase, Jr., J. Phys. Chem. Ref. Data **9**, 1 (1998).
[6] T. J. Buckley, R. D. Johnson III, R. E. Huie, Z. Zhang, S. C. Kuo, and R. B. Klemm, J. Phys. Chem. **99**, 4879 (1995).
[7] V. D. Knyazev, A. Benczura, and I. R. Slagle, J. Phys. Chem. A **101**, 849 (1997).
[8] D. A. Dixon and D. Feller, J. Phys. Chem. A **102**, 8209 (1998).
[9] M. R. Zachariah, P. R. Westmoreland, D. R. Burgess, Jr., W. Tsang, and C. F. Melius, J. Phys. Chem. **100**, 8737 (1996).
[10] D. E. Klimek and M. J. Berry, Chem. Phys. Lett. **20**, 141 (1973).
[11] Y. Ishikawa, K. Sugita, and S. Arai, Chem. Phys. Lett. **109**, 264 (1984).
[12] Y. S. Choi and C. B. Moore, J. Chem. Phys. **90**, 3875 (1989).
[13] Y. S. Choi, P. Teal, and C. B. Moore, J. Opt. Soc. Am. B **7**, 1829 (1990).
[14] Y. S. Choi and C. B. Moore, J. Chem. Phys. **94**, 5414 (1991).
[15] Y. S. Choi and C. B. Moore, J. Chem. Phys. **97**, 1010 (1992).
[16] Y. S. Choi and C. B. Moore, J. Chem. Phys. **103**, 9981 (1995).
[17] K. Saito, H. Kuroda, T. Kakumoto, H. Munechika, and I. Murakami, Chem. Phys. Lett. **113**, 399 (1985).
[18] B. R. Weiner and R. N. Rosenfeld, J. Phys. Chem. **92**, 4640 (1988).
[19] R. N. Dixon and T. W. R. Hancock, J. Phys. Chem. A **101**, 7567 (1997).
[20] C. L. Reed, M. Kono, S. R. Langford, T. W. R. Hancock, R. N. Dixon, and M. N. R. Ashfold, J. Chem. Phys. **106**, 6198 (1997).
[21] T. W. R. Hancock and R. N. Dixon, J. Chem. Soc., Faraday Trans. **93**, 2707 (1997).
[22] C. L. Reed, M. Kono, S. R. Langford, R. N. Dixon, and M. N. R. Ashfold, J. Chem. Soc., Faraday Trans. **93**, 2721 (1997).
[23] C. Maul, C. Dietrich, T. Haas *et al.*, Phys. Chem. Chem. Phys. **1**, 767 (1999).
[24] K. Morokuma, S. Kato, and K. Hirao, J. Chem. Phys. **72**, 6800 (1980).
[25] J. D. Goddard and H. F. Schaefer, J. Chem. Phys. **93**, 4907 (1990).
[26] K. Kamiya and K. Morokuma, J. Chem. Phys. **94**, 7287 (1991).
[27] J. S. Francisco and Y. Zhao, J. Chem. Phys. **96**, 7587 (1992).
[28] T.-G. Wei and R. E. Wyatt, J. Phys. Chem. **97**, 13580 (1993).
[29] T. Yamamoto and S. Kato, J. Chem. Phys. **107**, 6114 (1997).
[30] T. Yamamoto and S. Kato, J. Chem. Phys. **109**, 9783 (1998).
[31] T. Yamamoto and S. Kato, J. Chem. Phys. **112**, 8006 (2000).
[32] M. N. Glukhovstev and R. D. Bach, J. Phys. Chem. A **101**, 3574 (1997).
[33] S. Anand and H. B. Schlegel, J. Phys. Chem. A **106**, 11023 (2002).
[34] F. E. Budenholzer and T. Yu, J. Phys. Chem. A **102**, 947 (1998).
[35] R. Sumathi and A. R. Chandra, Chem. Phys. **165**, 257 (1992).
[36] H. Tachikawa, Phys. Chem. Chem. Phys. **1**, 2675 (1999).
[37] W.-H. Fang and R.-Z. Liu, J. Chem. Phys. **115**, 5411 (2001).
[38] C. C. Wang, Y. T. Lee, J. J. Lin, J. Shu, Y. Y. Lee, and X. Yang, J. Chem. Phys. **117**, 153 (2002).
[39] S.-H. Lee, Y.-Y. Lee, Y. T. Lee, and X. Yang, J. Chem. Phys. **119**, 827 (2003).
[40] J. J. Lin, Y. Chen, Y. Y. Lee, Y. T. Lee, and X. Yang, Chem. Phys. Lett. **361**, 374 (2002).
[41] G. A. Olah and S. J. Kuhn, J. Am. Chem. Soc. **82**, 2380 (1960).
[42] P. Erman, A. Karawajczyk, E. Rachlew-Kallne, C. Stromholm, J. Larsson, A. Persson, and R. Zerne, Chem. Phys. Lett. **215**, 173 (1993).
[43] J. M. Dyke, J. Chem. Soc., Faraday Trans. 2 **83**, 69 (1987).
[44] P. W. Tiedemann, S. L. Anderson, S. T. Ceyer, T. Hirooka, C. Y. Ng, B. H. Mahan, and Y. T. Lee, J. Chem. Phys. **71**, 605 (1979).
[45] L. E. Giddings, Jr. and K. K. Innes, J. Mol. Spectrosc. **6**, 528 (1961).
[46] L. E. Giddings, Jr. and K. K. Innes, J. Mol. Spectrosc. **8**, 328 (1962).